STM study of oxygen on Rh(110)

V. R. Dhanak,* K. C. Prince, and R. Rosei†
Sincrotrone Trieste, Padriciano 99, 34012 Trieste, Italy

P. W. Murray, F. M. Leibsle, M. Bowker,‡ and G. Thornton§
Interdisciplinary Research Centre in Surface Science, University of Liverpool, Liverpool L69 3BX, United Kingdom
(Received 26 July 1993; revised manuscript received 25 October 1993)

The $(2\times2)p2mg$ and $c(2\times2n)$ structures induced by oxygen adsorption on Rh(110) have been examined by means of scanning tunneling microscopy. The real-space images show the glide and centered symmetry required by the diffraction patterns, as well as substrate reconstruction. In addition, a metastable (6×2) structure and a number of defects have been identified and characterized, including an antiphase domain wall in the (2×2) structure. Where a step defect separates two $c(2\times8)$ domains, they tend to adopt a specific morphological relationship.

I. INTRODUCTION

Most fcc transition-metal (110) surfaces show a strong tendency to reconstruct, either spontaneously as in the cases of Au, Pt, and Ir, or in the presence of adsorbates for metals such as Pd, Ag, Cu, and Ni.[1] Oxygen adsorption on the (110) surfaces of Cu, Ni, and Ag, for instance, leads to a reconstruction with added rows of metal-oxygen-metal atoms in the $\langle 100\rangle$ direction, forming $(n\times1)$ structures.[2]

For the case of oxygen on Rh(110), a variety of surface structures have been reported, depending on the coverage and temperature of treatment.[3–5] Adsorption followed by annealing to 700 K results in three types of structures depending on the coverage: $(2\times3)pg$, $(2\times2)p2mg$, and $c(2\times2n)$ ($n=3$, 4, and 5), which correspond to coverages of 0.3, 0.5, and 0.6–1 ML, respectively, with the $c(2\times10)$ structure appearing at the highest coverage. Hydrogen reduction of these three types of structures at 370 K results, respectively, in (1×3), (1×2), and $(1\times n)$ O-free structures which are metastable and revert to (1×1) at temperatures above 480 K.[6] The structure of the (1×2) surface has been shown to be of the missing row type.[7] Electron energy loss spectroscopy (EELS) studies[8] were interpreted as being consistent with the structure models developed for the low-energy electron diffraction (LEED) studies. Taken together, these studies suggest that oxygen induces a $(1\times n)$ reconstruction of the rhodium substrate, which contrasts with the $(n\times1)$ oxygen-induced reconstructions observed on the (110) surfaces of Cu, Ni, and Ag.

In a previous paper,[9] we reported our first scanning tunnel microscope (STM) results concerning the adsorption of oxygen on Rh(110). The series of $c(2\times2n)$ structures, with $n=3$, 4, and 5, were imaged and we showed that these involve reconstruction of the substrate as had previously been hypothesized.[6] Structural models were proposed showing every nth close-packed row along the $\langle 110\rangle$ direction missing, with oxygen in the threefold coordinated sites along the troughs. With two equivalent sites within the substrate unit cell, the oxygen atoms form a zigzag chain along the troughs, doubling the size of the unit cell in the $\langle 110\rangle$ direction. In the present paper, we describe further scanning tunneling microscopy results for the $c(2\times2n)$ reconstructions, and present results for the Rh{110}$(2\times2)p2gm$-O structure.

II. EXPERIMENT

The STM measurements were made in an Omicron UHV instrument operated at a base pressure of $<10^{-10}$ mbar. The system is fitted with a preparation stage and a fast entry port for rapid introduction of samples. The main chamber is equipped with a retractable four-grid rear-view LEED-Auger retarding field analyzer. Sample annealing and argon-ion treatment could be performed in either the preparation chamber or the main chamber in front of the LEED optics. The STM is designed for room-temperature measurements with the tungsten tip held at ground potential and the sample biased. Imaging was carried out in the constant current mode. The tunneling parameters were varied over a wide range (typically, bias voltage 0.3–2 V positive and negative, and tunneling current 0.2–1.0 nA) with no appreciable difference to the images.

The measurements were performed on two different Rh(110) samples, which had previously been used for other measurements.[4,10] The crystals were of 99.99% nominal purity and were cut to within 0.5° of the (110) plane. They were cleaned by cycles of Ar-ion sputtering and annealing to 700–1200 K. Using this procedure, we obtained a clean surface as judged from the sharp (1×1) LEED and the characteristic Auger spectrum of clean rhodium. The $c(2\times6)$ and $c(2\times8)$ oxygen-induced structures were prepared by exposing the sample to 6 and 12 L of oxygen at 570 K, respectively, while observing the LEED pattern. Although the LEED patterns indicated either a $c(2\times6)$ or a $c(2\times8)$ pattern, STM showed that there were small domains of both structures as well as the $c(2\times10)$ reconstruction coexisting with the predominant structure (see below). The Rh{110}$(2\times2)p2mg$-O structure was obtained by expos-

 ©1994 The American Physical Society

ing the sample to about 1.5 L of NO at 450 K and flashing to 800 K. Previous studies have shown that this procedure results in a nitrogen-free oxygen-induced $(2\times2)p2mg$ structure with half monolayer coverage.[11] The LEED patterns were examined before and after imaging in the STM and were found to have remained unchanged during the measurement, indicating the stability of these structures.

III. RESULTS

Figure 1 shows an area of the $c(2\times6)$ structure imaged with higher resolution than in our previous report. Darker areas are lower and lighter areas are raised. The missing rows are clearly visible as black stripes and the remaining rows display a zigzag structure. For small tip-surface distances, oxygen is usually imaged in STM as a depression, even if the atom is located above the surface as in the case of oxygen adsorbed on Ni.[12] This is due to the low density of states near the Fermi level on the oxygen atom, compared with that on a metal. Under the conditions used in our work we therefore expect that oxygen atoms appear dark, if they are imaged.

The zigzag structure of the image may therefore be interpreted as being due to bright Rh atoms and dark oxygen atoms, in which case the structure is in general agreement with our model in which the oxygen atoms are placed in zigzag rows in the troughs. However, since in STM it is not always possible to distinguish topographic contrast from electronic structure contrast, the zigzag structure may alternatively be due to a zigzag displacement of the Rh atoms. If the contrast were entirely topographic and due to displacement of the Rh atoms, the maximum lateral shift would be 0.7 Å, which seems unreasonably large. However, the troughs do not have a zigzag structure, but instead have a local plane of reflection symmetry. This indicates that the atoms in the trough are not, in fact, arranged in a zigzag fashion. In our previous paper,[9] it was not possible to draw this conclusion because thermal drift distorted the image slightly. Furthermore, the zigzag structures on adjacent rows are seen to be in antiphase, an observation which was also not possible with the earlier data.

In one set of experiments the sample was annealed to only 670 K following Ar-ion bombardment with the result that the structure contained a number of defects. The result of oxygen adsorption on this surface, which displayed a $c(2\times8)$ LEED pattern, is shown in Figs. 2(a) and 2(b). The segmented structures marked *A* are in-

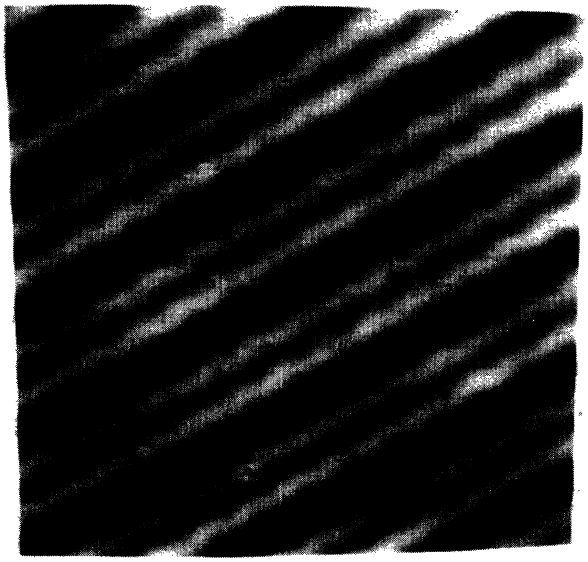

FIG. 1. A 60×60 Å^2 image of the $c(2\times6)$ phase, recorded at a sample bias of $+2$ V and tunneling current of 1 nA. Bright rows are parallel to the substrate ⟨110⟩ direction.

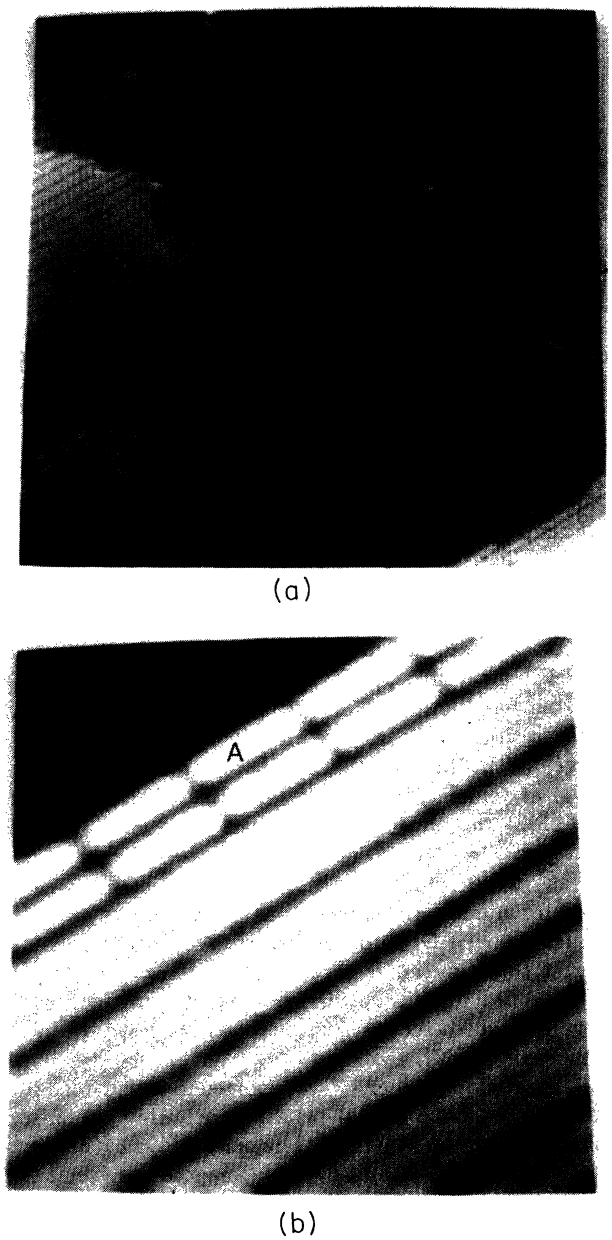

FIG. 2. (a) Large area (500×500 Å^2) showing a variety of oxygen-induced structures and defects on Rh(110). This image was recorded at -2 V, 1 nA. (b) 100×100 Å^2 high-resolution image showing the segmented structures (*A*) at a step edge, recorded at -2 V, 1 nA. The bright rows are parallel to the ⟨110⟩ direction.

teresting: where the resolution was adequate, each segment was found to be composed of six zigzag features each about 3 Å in length, but occasionally five or seven such features were also observed. The local structure therefore appears to be one unit cell of a (6×2) or $c(6\times4)$ structure, depending on whether the deep troughs also contain zigzag rows of oxygen atoms. These segmented structures were always observed as a minor phase on the surface and usually, but not always, at step edges. Line scans indicate that the dark bands between segments (in the $\langle 110\rangle$ direction) correspond to a corrugation of 0.9 Å, which is consistent with the absence of a Rh atom from the row. We tentatively interpret the segmented structure as being due to a metastable phase which forms during the conversion from (1×1) to $c(2\times2n)$, and is associated largely with steps edges.

A large area image of the Rh{110}$(2\times2)p2mg$-O structure is shown in Fig. 3, and the higher magnification image in Fig. 4 illustrates a local zigzag structure very similar to that observed in images of the $c(2\times6)$ phase. The same comment concerning contrast mechanism holds, i.e., we believe the contrast to be due to bright Rh atoms and dark oxygen atoms. The cell dimensions of this structure and those of the $c(2\times6)$ structure, derived from the STM images, are within 10% of the expected value; this discrepancy is attributed to thermal drift. The corrugation measured from current height profiles taken along the two principal directions of the surface are summarized in Table I for the five different Rh(110)-O phases.

In Fig. 4, a defect marked by the line is interpreted as an antiphase domain wall: the structure below this line is displaced by about 2.5 Å parallel to the rows with respect to the structure above it. This is the kind of defect that has been associated with the $(2\times2)\rightarrow(1\times2)$ phase transition at 850 K in this system.[10] A structural model is shown in Fig. 4(b), indicating the two domains of the $(2\times2)p2mg$ phases separated by an antiphase boundary running along the $\langle 110\rangle$ direction. Recently, a method of describing linear defects by means of surface Burgers vectors has been reported,[13] and this forms a useful basis for labeling and distinguishing defects. The present linear defect can be labeled as having a Burgers vector $a/\sqrt{2}[100]$, where a is the lattice parameter of Rh, and the x direction is along the rows of atoms.

In Fig. 3, a number of dark stripes or furrows are evident on the broad $(2\times2)p2mg$-O terraces, and a typical area in which some of these defects meet a step is shown in Fig. 5(a). Line scans indicate that the width of these furrows is 11–12 Å, which is consistent with a local (1×3) structure, while the step has a measured height of

FIG. 3. Large area (700×800 Å^2) image of the Rh{110}$(2\times2)p2mg$-O structure, taken at -2 V, 1 nA.

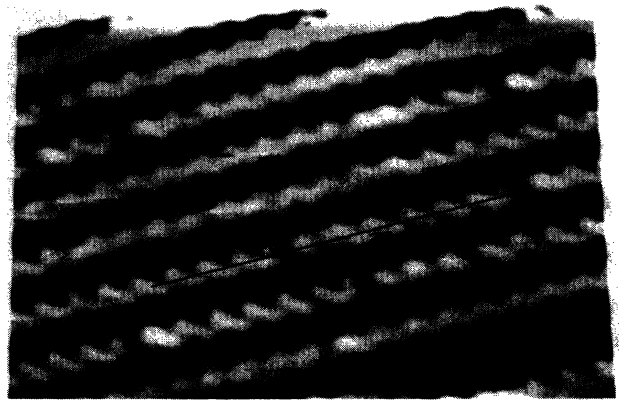

(a)

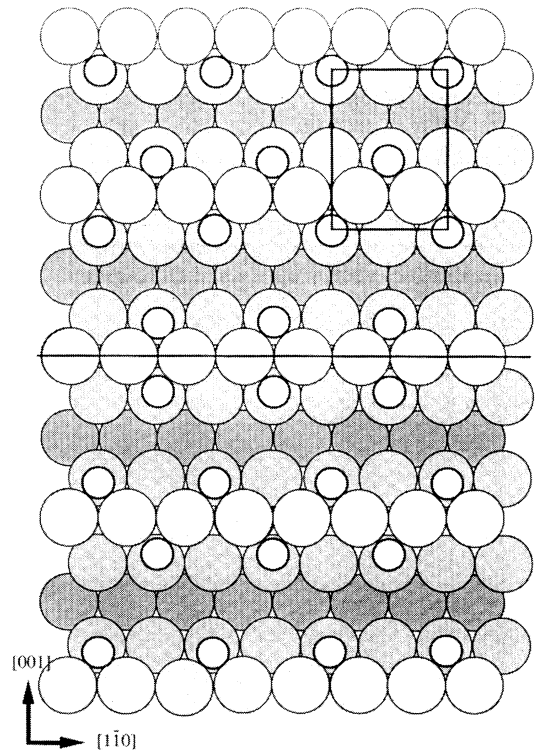

(b)

FIG. 4. (a) High-resolution image (70×100 Å^2) of the $(2\times2)pg$ structure. The line indicates a defect. The bright rows are parallel to the $\langle 110\rangle$ direction. (b) Structural model of the image in (a), showing an antiphase domain boundary along $\langle 110\rangle$ (from Ref. 10, with modifications). Large shaded circles represent Rh atoms, with lighter shades corresponding to higher atoms. The open circles represent oxygen atoms. The $(2\times2)p2mg$ unit cell is outlined.

TABLE I. Corrugation (in Å) from the current height profiles.

Structure	Corrugation in the missing rows along ⟨100⟩ ⟨110⟩	Corrugation on the terraces (ridges for 2×2) along ⟨100⟩ and ⟨110⟩
$c(2\times6)$	0.7±0.2	0.16±0.02
	0.18±0.03	0.09±0.02
$c(2\times8)$	0.8±0.2	0.14±0.03
	0.2±0.05	0.09±0.02
$c(2\times10)$	0.7±0.2	0.11±0.03
	0.16±0.04	0.09±0.03
$(2\times2)p2mg$	0.82±0.1	
	0.18±0.07	0.27±0.07
Segmented	1.4±0.2	
	0.9±0.1	0.1±0.02

1.5–1.6 Å, i.e., it is a monatomic step. Comparing the rows of atoms above and below the step, the rows in area *A* (the upper terrace) are displaced towards the bottom of the image relative to those of area *B*. However, the rows in area *A* are displaced towards the top of the image relative to the rows in area *C*, which implies that the furrow between areas *B* and *C* causes a displacement. Again the situation can be summarized succinctly using Burgers vector notation. In Fig. 5(b) the defects and their respective Burgers vectors are sketched. The step begins at the top of the figure with a Burgers vector $\mathbf{b}_2 = a/2\sqrt{2}[-111]$ for the *x* axis along the rows, and the *y* axis perpendicular to the rows, with the *z* axis perpendicular to the surface. The step coalesces with the furrow which has a Burgers vector $\mathbf{b}_1 = a\,[0\,1\,0]$ to give

$$\mathbf{b}_3 = a[-1/2\sqrt{2}\;\; 1+1/2\sqrt{2}\;\; 1/2\sqrt{2}]\ .$$

The linear defect between areas *A* and *D* then adds a further $\mathbf{b}_1 = a\,[010]$ to give

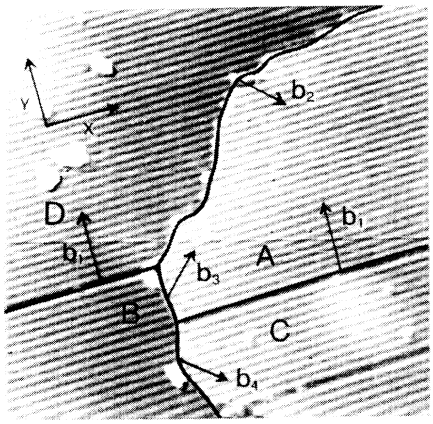

FIG. 5. A 500×500 Å^2 image of the $(2\times2)p2mg$-O structure, taken at −2 V, 1 nA. A map of the defects is outlined, with letters indicating the region separated by defects, and arrows indicating the Burgers vectors of the different regions. Bright rows are parallel to the ⟨110⟩ direction.

$$\mathbf{b}_4 = a[-1/2\sqrt{2}\;\; 2+1/2\sqrt{2}\;\; 1/2\sqrt{2}] = a/2\sqrt{2}[-1\;1\;1]$$

since the Burgers vector is defined modulo a surface lattice vector, *a* [0 2 0].

Another observation with regard to defects concerns steps in the $c(2\times2n)$ structures. The missing rows, in general, tend to line up on crossing a step as seen in Fig. 6: they cannot be exactly in line because there is always a lateral displacement at the step, but there is a tendency for the missing rows on either side of the step to be as close as possible. If there were no relationship between the domains on the different terraces, a random distribution of all possible separations between the missing rows on the two terraces would be expected. Since the step is a kind of surface dislocation, the Burgers vector formalism represents a convenient way of summarizing and classifying the relationship between the two domains. On the (1×1) surface, for instance, a step Burgers vector is of type $a/2\sqrt{2}[1\;1\;1]$, as stated above. For a $c(2\times8)$ structure, the additional Burgers vectors due to a step plus a lateral displacement are of the type $a/2\sqrt{2}[1\;1+m2\sqrt{2}\;1]$, where $m=0$, 1, 2, or 3. For two regions of the $c(2\times8)$ structure nucleated at random and separated by a step, all of these four Burgers vectors should occur with equal frequency. However, $m=0$ Burgers vectors occur predominantly (approximately 70%, with the remainder having predominantly $m=1$, see Table II), suggesting that, after growth, the structures on neighboring terraces tend to adopt a specific morphological relationship. We call this a "translational relationship" between domains and it appears to be analogous to an effect well known in solid-state structural physics, the existence of preferred orientation relationships. This gives rise to preferred angular relationships between crystallites of the same or different phases. In

FIG. 6. A 1000×1000 Å^2 image of the Rh{110}-$c(2\times8)$ structure with steps. Note that the missing rows, which appear as dark lines on the terraces, tend to align across steps, as indicated by the arrows. Bright rows are parallel to the ⟨110⟩ direction.

TABLE II. Measurement of the alignment of missing rows in the $c(2\times8)$ structure across step edges. The integer m refers to lateral displacement in the vector $a/2\sqrt{2}[1\ 1+m2\sqrt{2}\ 1]$.

Burgers vector displacement m	Number of measurements
$m=0$	31
$m=1$	10
$m=2$	3

two dimensions, however, the orientations are fixed by the substrate, and only translational freedom is allowed.

IV. DISCUSSION

As stated above, the contrast in the zigzag structures may arise from topographic or electronic structure effects and therefore a bond length cannot be extracted. However, the results support the original model for this group of oxygen-induced structures,[5,6] but with some modification. The fundamental ideas are that oxygen induces a missing row reconstruction of the substrate, and generally adsorbs in zigzag rows in troughs. At a coverage of one half monolayer, this is a (1×2) substrate reconstruction and all of the oxygen is adsorbed in the troughs. Recent quantitative LEED analysis has shown that the oxygen is adsorbed in threefold coordinated sites at the top of the (111) microfacets of the missing rows,[14,15] as shown in Fig. 4(b). The images show this glide structure clearly for the $(2\times2)p2mg$ phase, although it is not possible to determine the origin of the contrast. We can exclude the possibility that the Rh atoms are displaced slightly on the basis of the LEED structure determination.[14,15]

As the coverage is increased, the number of missing row is reduced from every second row to one out of n, to give unreconstructed terraces of width $n-1$ rows between the missing rows. These terraces also contain troughs, which are not as deep as the missing row troughs, but can accommodate more oxygen. The motif of zigzag rows of oxygen is continued on these small terraces as seen in Fig. 1. There are two possible ways of arranging the zigzag lines: with those in adjacent troughs in phase, or in antiphase. In our original model,[9] it was suggested that they were in antiphase, and this is confirmed by the present images. The deep troughs do not show a zigzag pattern, but instead are planes of mirror symmetry with a periodicity double that of the clean surface. This implies that the previous model has to be modified, and a quantitative LEED study has been undertaken for this purpose. The corrugation in the missing rows for the $c(2\times2n)$ structures is close to that measured for the $(2\times2)p2mg$ structure (Table I), which suggests that the oxygen site is similar for these structures.

The origin of the near-alignment of missing rows across the steps in the $c(2\times2n)$ structures, Fig. 6, is reminiscent of the effect reported by Kern *et al.*[16] who observed that large period superlattices continued across steps for the O/Cu(110) system. The origin of the effect in the present system may lie either in the kinetics of growth or in the interaction between the terraces in equilibrium. For example, the missing row troughs may act during growth as preferred channels for diffusion, analogous to pipe diffusion in dislocated solids. Adjacent regions separated by a step will then show faster growth if the missing row troughs are nearly aligned, and will thus form a larger fraction of the surface. Alternatively, the origin may be an equilibrium rather than a kinetic effect, as postulated by Kern *et al.* for O/Cu(110). Interactions between the terraces, e.g., mediated by long-range strain fields, may minimize the total energy when the missing rows are nearly aligned. Considered from the point of view of surface dislocations, it is clear that the different relative positions of the missing rows on adjacent terraces produce dislocations of different Burgers vectors, as discussed above. Furthermore, it is *a priori* evident that their energies will be different: the experiment shows that these energies are significantly different.

The corrugation heights observed at points or "holes" where Rh atoms are missing are compared in Table I. It is noticeable that in the segmented structure, the apparent corrugation of 1.4 Å in the $\langle 100\rangle$ direction is much larger than that observed for the other structures. This suggests that the holes from which the Rh atoms are missing contain oxygen atoms since, as noted above, oxygen is usually imaged as a depression in STM.

V. SUMMARY

The $(2\times2)p2mg$ and $c(2\times2n)$ phases of Rh{110}-O have been imaged. The results support some aspects of the structural models previously put forward, which consist of a missing row substrate with zigzag rows of oxygen atoms. Some minor modifications to the models may be necessary for the $c(2\times2n)$ structures as the site of the oxygen is not definite. In addition, a variety of defects have been observed, of which the antiphase domain boundary in the $(2\times2)p2mg$ structure, with surface Burgers vector a [1 0 0], had been predicted previously. Domains of the $c(2\times2n)$ structure separated by a step do not adopt a random relative orientation, but tend to have the missing row troughs aligned, to give a "translational relationship" between domains.

*Also at INFM-TASC, Padriciano 99, 34012 Trieste, Italy.
†Also at Dipartimento di Fisica, Università di Trieste, 34000 Trieste, Italy.
‡Present address: Department of Chemistry, University of Reading, Reading RG6 2AD, UK.
§Also at Department of Chemistry, University of Manchester, Manchester M13 9PL, UK.

[1] S. P. Chen and A. F. Voter, Surf. Sci. **244**, L107 (1991), and references therein.
[2] D. J. Coulman, J. Wintterlin, R. J. Behm, and G Ertl, Phys. Rev. Lett. **64**, 1761 (1990), and references therein; Y. Kuk, P. J. Silverman, and H. Q. Nguyen, *ibid.* **59**, 1452 (1987); I.

Stensgaard, L. Ruan, F. Besenbacher, F. Jensen, and E. Laegsgaard, Surf. Sci. **269/270**, 81 (1992), and references therein.

[3]E. Schwarz, H. Lenz, H. Wohlgemuth, and K. Christmann, Vacuum **41**, 167 (1990).

[4]M. Bowker, Q. Guo, and R. Joyner, Surf. Sci. **253**, 33 (1991).

[5]G. Comelli, V. R. Dhanak, M. Kiskinova, G. Paolucci, K. C. Prince, and R. Rosei, Surf. Sci. **269/270**, 360 (1992); **260**, 7 (1992).

[6]V. R. Dhanak, G. Comelli, G. Cautero, G. Paolucci, K. C. Prince, M. Kiskinova, and R. Rosei, Chem. Phys. Lett. **188**, 237 (1992).

[7]A. Bellman, A. Morgante, M. Polli, F. Tommasini, D. Cvetko, V. R. Dhanak, A. Lausi, K. C. Prince, and R. Rosei, Surf. Sci. (to be published).

[8]D. Alfè P. Rudolf, M. Kiskinova, and R. Rosei, Chem. Phys. Lett. **211**, 220 (1993).

[9]P. W. Murray, F. M. Leibsle, Y. Li, Q. Guo, M. Bowker, G. Thornton, V. R. Dhanak, K. C. Prince, and R. Rosei, Phys. Rev. B **47**, 12 976 (1993).

[10]A. Bellman, D. Cvetko, A. Morgante, M. Polli, F. Tommasini, K. C. Prince, and R. Rosei, Surf. Sci. Lett. **281**, L321 (1993).

[11]M. Kiskinova, G. Comelli, S. Lizzit, G. Paolucci, and R. Rosei, Appl. Surf. Sci. **64**, 185 (1993).

[12]J. Behm, *Scanning Tunneling Microscopy I,* Springer Series in Surface Sciences Vol. 20, edited by H.-J. Güntherodt and R. Wiesendanger (Springer-Verlag, Berlin, 1992).

[13]K. C. Prince, A. Morgante, D. Cvetko, and F. Tommasini, Surf. Sci. **297**, 235 (1993).

[14]M. Gierer, H. Over, G. Ertl, H. Wohlgemuth, E. Schwarz, and K. Christmann, Surf. Sci. Lett. (to be published).

[15]C. Comicioli, V. R. Dhanak, G. Comelli, A. Astaldi, K. C. Prince, R. Rosei, A. Atrei, and E. Zanazzi, Chem. Phys. Lett. **214**, 438 (1993).

[16]K. Kern, H. Niehus, A. Schatz, P. Zeppenfeld, J. George, and G. Comsa, Phys. Rev. Lett. **67**, 855 (1991).

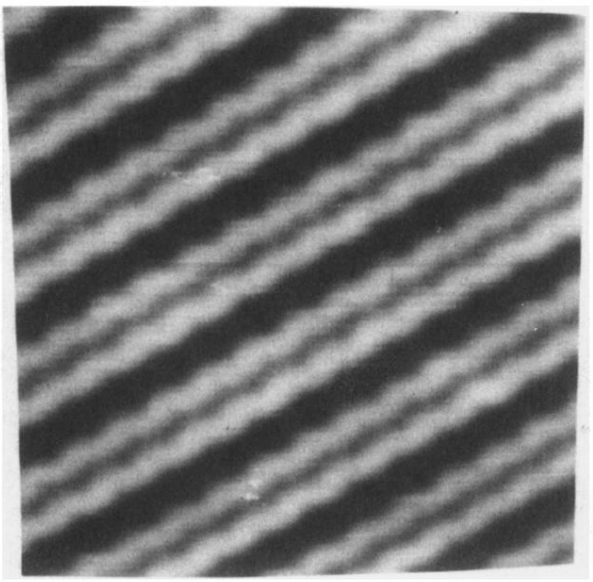

FIG. 1. A 60×60 Å^2 image of the $c(2 \times 6)$ phase, recorded at a sample bias of $+2$ V and tunneling current of 1 nA. Bright rows are parallel to the substrate $\langle 110 \rangle$ direction.

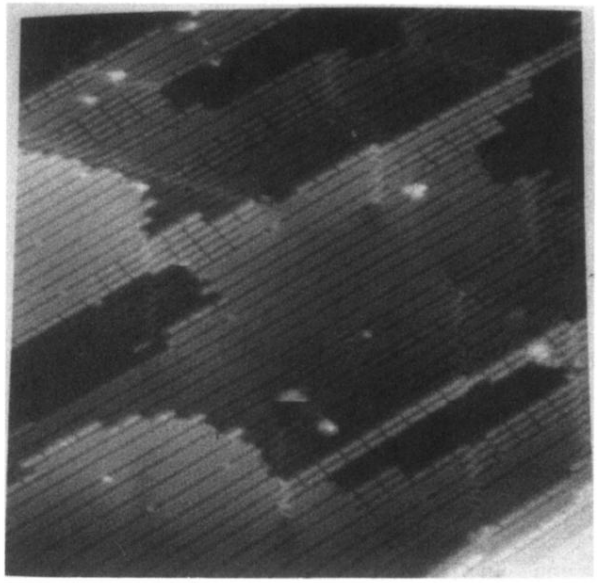

(a)

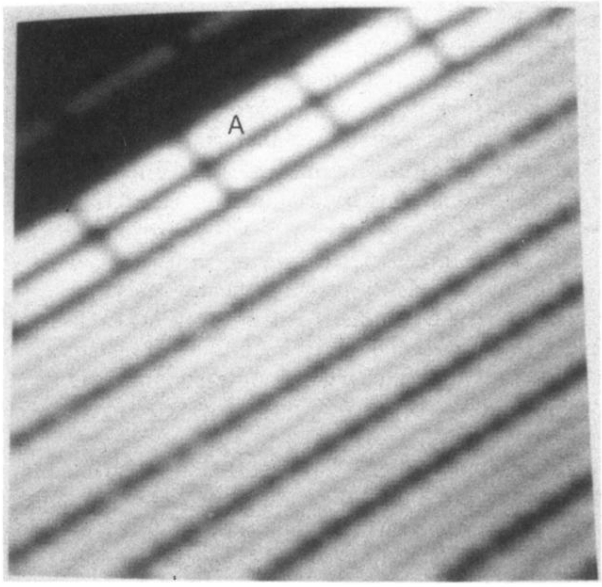

(b)

FIG. 2. (a) Large area (500×500 Å^2) showing a variety of oxygen-induced structures and defects on Rh(110). This image was recorded at -2 V, 1 nA. (b) 100×100 Å^2 high-resolution image showing the segmented structures (A) at a step edge, recorded at -2 V, 1 nA. The bright rows are parallel to the $\langle 110 \rangle$ direction.

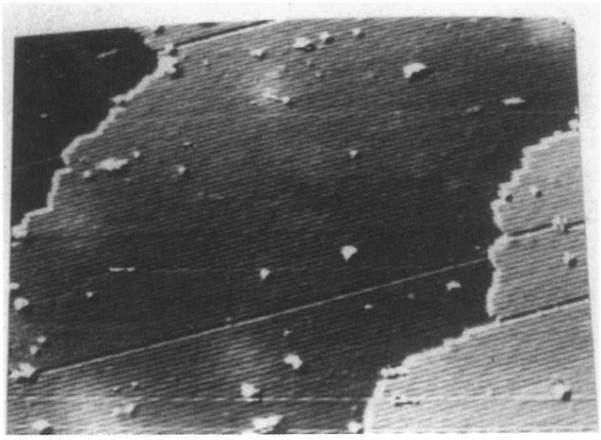

FIG. 3. Large area (700×800 Å^2) image of the Rh{110}$(2\times2)p2mg$-O structure, taken at -2 V, 1 nA.

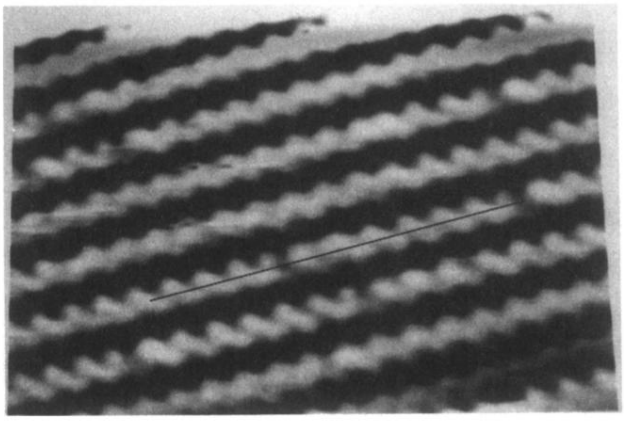

(a)

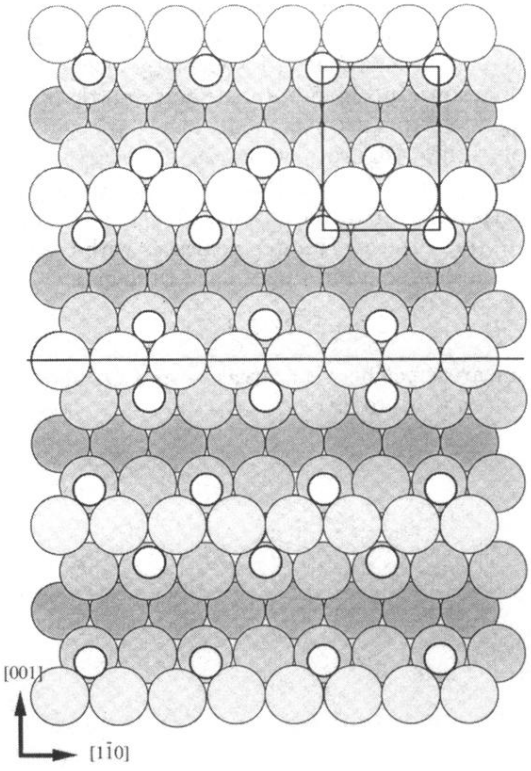

(b)

FIG. 4. (a) High-resolution image (70×100 Å^2) of the $(2\times2)pg$ structure. The line indicates a defect. The bright rows are parallel to the $\langle 110\rangle$ direction. (b) Structural model of the image in (a), showing an antiphase domain boundary along $\langle 110\rangle$ (from Ref. 10, with modifications). Large shaded circles represent Rh atoms, with lighter shades corresponding to higher atoms. The open circles represent oxygen atoms. The $(2\times2)p2mg$ unit cell is outlined.

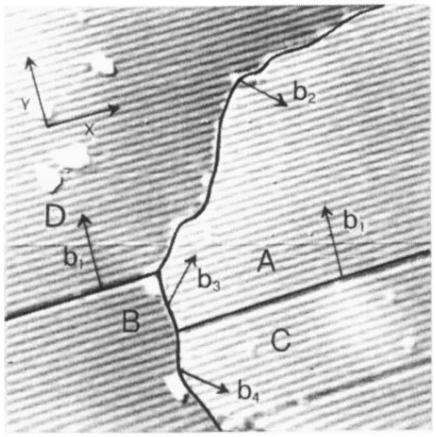

FIG. 5. A 500×500 Å^2 image of the $(2\times2)p2mg$-O structure, taken at -2 V, 1 nA. A map of the defects is outlined, with letters indicating the region separated by defects, and arrows indicating the Burgers vectors of the different regions. Bright rows are parallel to the $\langle 110 \rangle$ direction.

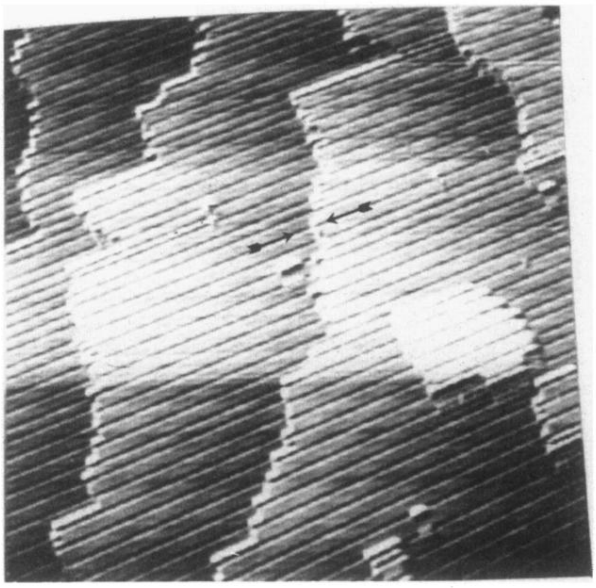

FIG. 6. A 1000×1000 Å^2 image of the Rh{110}-$c(2 \times 8)$ structure with steps. Note that the missing rows, which appear as dark lines on the terraces, tend to align across steps, as indicated by the arrows. Bright rows are parallel to the ⟨110⟩ direction.